Li, X., Li, X., Ma, F., Yuan, Y., Zhang, K., Zhou, F., Zhang, X. (2019): Improved PPP Ambiguity Resolution with the Assistance of Multiple LEO Constellations and Signals. - *Remote Sensing*, *11*, 4.

DOI: http://doi.org/10.3390/rs11040408

*remote sensing*

MDPI

*Article*

# Improved PPP Ambiguity Resolution with the Assistance of Multiple LEO Constellations and Signals

**Xin Li [1], Xingxing Li [1,2,*], Fujian Ma [1], Yongqiang Yuan [1], Keke Zhang [1], Feng Zhou [3] and Xiaohong Zhang [1]**

1 School of Geodesy and Geomatics, Wuhan University, Wuhan 430079, China; lixinsgg@whu.edu.cn (X.L.); fjmasgg@whu.edu.cn (F.M.); yqyuan@whu.edu.cn (Y.Y.); kkzhang@whu.edu.cn (K.Z.); xhzhang@sgg.whu.edu.cn (X.Z.)

2 German Research Centre for Geosciences GFZ, Telegrafenberg, 14473 Potsdam, Germany

3 College of Geomatics, Shandong University of Science and Technology, Qingdao 266590, China; zhouforme@163.com

* Correspondence: lxlq109121@gmail.com

Received: 15 January 2019; Accepted: 13 February 2019; Published: 17 February 2019


**Abstract:** The fusion of low earth orbit (LEO) constellation and Global Navigation Satellite Systems (GNSS) can increase the number of visible satellites and optimize spatial geometry, which is expected to improve the performance of precise point positioning (PPP) ambiguity resolution (AR). In addition, the multi-frequency signals of LEO satellites can bring a variety of observation combinations, which is potential to further improve the efficiency of PPP AR. In this contribution, multi-frequency PPP AR was achieved with the augmentation of different LEO constellations. Three types of LEO constellations were designed with 60, 192, and 288 satellites. Moreover, the corresponding observation data were simulated with the GNSS observations over the ground stations. The LEO constellations were designed to transmit navigation signals on three frequencies: L1, L2, and L5 at 1575.42, 1227.6, and 1176.45 MHz, respectively, which are consistent with the GPS signals. For PPP AR, the uncalibrated phase delay (UPD) products of GNSS and LEO were estimated first. Furthermore, the quality of UPD products was also analyzed. The research findings show that the performance of estimated LEO UPD is comparable to that of GNSS UPD. Based on the UPD products, LEO-augmented multi-GNSS PPP AR can be achieved. Numerous results show that the performance of single-system and multi-GNSS PPP AR can be significantly improved by introducing the LEO constellations. The augmentation performance is more remarkable in the case of increasing LEO satellites. The time to first fix (TTFF) of the GREC fixed solution can be shortened from 7.1 to 4.8, 1.1, and 0.7 min, by introducing observations of 60-, 192-, and 288-LEO constellations, respectively. The positioning accuracy of multi-GNSS fixed solutions is also improved by about 60%, 80%, and 90% with the augmentation of 60-, 192-, and 288-LEO constellations, respectively. Compared to the dual-frequency solutions, the triple-frequency LEO-augmented PPP fixed solution presents a better performance. The TTFF of GREC fixed solutions is shortened to 33 s with the augmentation of 288-LEO constellation under the triple-frequency environment. It is worth indicating that the 288-satellite LEO-only PPP AR was conducted in dual-frequency and triple-frequency modes, respectively. The averaged TTFFs of both modes are 71.8 s and 55.2 s, respectively. It indicates that LEO constellation with 288 satellites is capable of achieving high-precision positioning independently and shows an even better performance than GNSS-only solutions.

**Keywords:** LEO constellation; precise point positioning (PPP); ambiguity resolution; multi-frequency; time to first fix (TTFF); positioning accuracy

## 1. Introduction

Traditional precise point positioning (PPP) [1,2] still suffers from the problem of a long initialization time to achieve a centimeter-level positioning accuracy, which also limits the wider application of PPP in some time-critical applications, such as precision agriculture, tsunami and earthquake warning, etc. To shorten the initialization time and improve the positioning accuracy, PPP ambiguity resolution (AR) has been proposed in recent years [3–7]. After the employment of AR, the positioning error of GPS PPP can converge to 5 cm in the three components within 30 min [8].

With the rapid development of multiple Global Navigation Satellite Systems (multi-GNSS), it is anticipated that more than 120 navigation satellites will offer a precise positioning service to all ranges of users by 2020 [9]. To assess the precise positioning performance with current multi-constellation GNSS, observation data of Multi-GNSS Experiment (MGEX) and BeiDou Experimental Tracking Network (BETN) networks were employed by Li et al. [9,10]. It has been confirmed that the performance of PPP in terms of convergence, accuracy, continuity, and reliability can be significantly improved by the fusion of multi-GNSS [9,11,12]. The convergence time of GPS-only PPP can be shortened by 70% when GLONASS, BDS, and Galileo observations are added, while the positioning accuracy is improved by about 25% [9]. For PPPAR, the time to first fix (TTFF) and positioning accuracy can also be improved by the fusion of multi-GNSS. The positioning accuracy of the GCRE fixed solution within 10 min is (1.84, 1.11, 1.53) cm, while the GPS-only result is (2.25, 1.29, 9.73) cm for the east, north, and vertical components [13]. Under a multi-frequency environment, the joint of the extra frequencies brings more combinations of signals, which could potentially further improve the performance of PPP AR. Geng et al. [14] demonstrated that triple-frequency PPP can achieve a successful ambiguity resolution within a few minutes based on the simulated data. Gu et al. [15] and Li et al. [16,17] performed triple-frequency PPP AR based on raw observations of GPS, BDS, and Galileo, respectively. Their results indicated that the third frequency could lead to an improvement in the PPP accuracy during the initialization phase.

Currently, the era of low earth orbit (LEO) constellation is coming. Some famous international enterprises, such as American OneWeb, SpaceX, and Boeing, have announced that they will launch and develop their commercial LEO constellations consisting of hundreds or thousands of satellites [18–20]. These LEO satellites can not only provide broadband Internet and communication services on the world scale, but also serve as navigation constellations, broadcasting navigation signals and providing a positioning, navigation, and timing (PNT) service. The navigation function has also been confirmed in the 66-satellite Iridium system, the only current LEO network with constant global coverage. Compared to the GNSS satellites located at medium or high orbit, LEO satellites take advantage of a lower orbit altitude and stronger signal strength, which is expected to achieve high-precision positioning in severely occluded areas [21]. At the same time, the LEO satellite has a fast motion and thus the spatial observation geometry changes rapidly, which provides an opportunity to solve the problem of a too long convergence time of PPP. In addition, the LEO satellite usually employs a polar orbit or near-polar orbit, and thus many visible satellites in high-latitude areas can be observed, which can improve the navigation and positioning accuracy in these regions. To demonstrate the contribution of LEO to GNSS, many researchers conducted numerous experiments about LEO-augmented high-precision positioning based on the simulated LEO observations. Ke et al. [22] found that with the inclusion of the LEO satellites, the convergence time of the GPS-only PPP decreased by 51.31%. The results of Ge et al. [23] show that LEO-augmented GNSS (GPS+BDS+Galileo) can decrease the PPP convergence time to 5 min. Li et al. [24] investigated the performance of LEO-augmented multi-GNSS (GPS + GLONASS + BDS + Galileo) PPP with different LEO constellations. The results indicated that more LEO satellites lead to a shorter convergence time and the convergence time can be shortened from 8.2 to 0.8 min by introducing observations from 288 polar-orbiting LEO satellites.

As previous studies all focused on the contribution of the LEO constellation to dual-frequency GNSS float solutions, in this paper, for the first time, multi-frequency LEO-augmented GNSS PPP

ambiguity resolution was investigated. The augmentation performance of different LEO constellations was evaluated in terms of TTFF and positioning accuracy. The benefits of multi-frequency LEO observations for PPP AR were also analyzed. After this introduction, this paper is organized as follows: the constellation design, data simulation, and LEO-augmented PPP AR methods are introduced in Section 2. Then, the results of uncalibrated phase delay (UPD) products, and the performance of the GNSS PPP AR with multiple LEO constellations and signals are evaluated in Section 3. Finally, the discussions and conclusions are provided in Sections 4 and 5, respectively.

## 2. Data and Methods

### *2.1. Constellation Design and Data Simulation*

In order to investigate the performance of LEO-augmented PPP AR, three types of LEO constellations were designed using Satellite Tool Kit (STK) software, which is commercial analytical software applied for the aerospace industry, developed by Analytical Graphics [25]. The satellite number was designed to be 60, 192, and 288, respectively. The altitude of the LEO satellite is 1000 km and the inclination is 90°. The polar orbits, which pass over the north and south poles of the earth and have the capability of covering different parts of the earth's surface, were adopted here.

Apart from the LEO observations, the GNSS observations were also simulated in this paper since the BDS and Galileo have not been fully completed. The GNSS constellation is designed based on their nominal parameter configurations [26–29]. Therefore, the satellite number of GPS, GLONASS, Galileo, and BDS was set as 24, 24, 30, and 35, respectively. All satellites of GPS, GLONASS, and Galileo were distributed over a medium earth orbit (MEO), while BDS consists of five geostationary Earth orbiting (GEO) satellites, three inclined geosynchronous orbiting (IGSO) satellites, and 27 MEO satellites. Twenty-four GPS MEO satellites are distributed in six orbital planes, while the GLONASS, Galileo, and BDS MEO satellites employ a Walker 24/3/1 constellation geometry. The orbit altitudes of GPS, GLONASS, and Galileo satellites are 20,180, 19,100, and 23,220 km, respectively. For BDS, the orbit altitude of the MEO satellite is 21,528 km, while GEO and IGSO satellites distribute on the orbit of the same altitude (35,786 km) with different inclinations (0° and 55°). The simulated GNSS and LEO constellations are plotted in Figure 1. Compared to the GNSS satellites, the LEO satellites are much closer to the Earth's surface because of the lower orbit altitude. It can also be found that more LEO satellites can be observed in the high-latitude region than the low-latitude region because the polar orbit is employed.

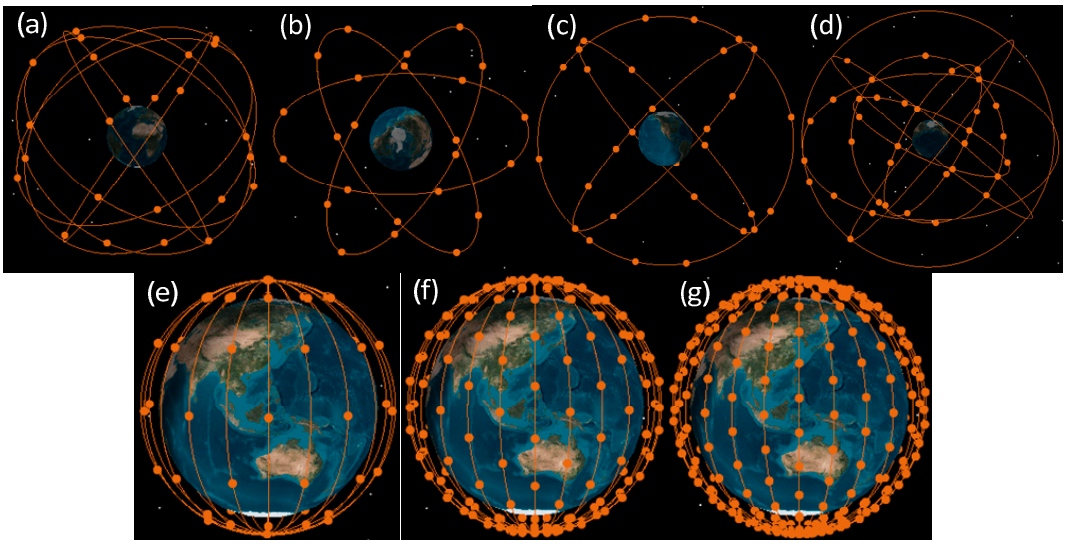


**Figure 1.** GNSS and designed LEO constellations. (**a**) GPS; (**b**) GLONASS; (**c**) Galileo; (**d**) BDS; (**e**) 60 LEO; (**f**) 192 LEO; (**g**) 288 LEO.

Observations of the GNSS and LEO satellites can be simulated based on the original phase and pseudorange observation equations ($L^s_{r,j}$ and $P^s_{r,j}$) as follows [30]:

$$L^s_{r,j} = \rho^s_{rg} + c(t_r - t^s) + \lambda_j(B_{r,j} - B_j{}^s) + \lambda_j N^s_{r,j} - I^s_{r,j} + T^s_r + \varepsilon^s_{r,j} \quad (1)$$

$$P^s_{r,j} = \rho^s_{rg} + c(t_r - t^s) + c(b_{r,j} - b_j{}^s) + I^s_{r,j} + T^s_r + e^s_{r,j} \quad (2)$$

where the indices $s$, $r$ and $j$ refer to the satellite, receiver, and carrier frequency, respectively; $t^s$ and $t_r$ are the clock offsets of the satellite and receiver, respectively; $c$ is the speed of the light; and $b_{r,j}$ and $b_j{}^s$ are the code hardware delay at the receiver and satellite sides, respectively. The receiver-dependent hardware delays are different from the individual systems and the difference is always called the inter-system bias (ISB) or inter-frequency bias (IFB, for GLONASS). $I^s_{r,j}$ and $T^s_r$ refer to the ionospheric delay and tropospheric delay, respectively; $N^s_{r,j}$ is the phase ambiguity; $B_{r,j}$ and $B_j{}^s$ refer to phase delay of the receiver and satellite, respectively; $\rho^s_{rg}$ is the geometric distance from the satellite to receiver; and $e^s_{r,j}$ and $\varepsilon^s_{r,j}$ denote the sum of measurement noise and multipath error for the code and carrier phase observations, respectively.

The process of data simulation is generating observations by the geometric distance from the satellite to receiver and a variety of errors. The static PPP was conducted before the simulation to obtain the receiver clock offset ($t_r$), the inter-system biases, and the zenith wet delay of the troposphere. The orbit of satellites is obtained from the Satellite Tool Kit software. The satellite clock is obtained from the IGS precise clock products. The new GNSS satellites and LEO satellites will use clock offsets of old satellites randomly. With the position of the satellite and receiver, the geometric distance between the receiver and satellites can be calculated. The dry part of tropospheric delays was calculated by empirical models—the Saastamoinen model in this study [31]. The phase center offsets (PCOs) and variations (PCVs) and tidal loading can be calculated according to the existing models [32]. The ionospheric delay was computed based on the mapping function and total electron content (TEC) provided by CODE's global ionosphere maps (GIM) [33]. The code bias of each frequency is simulated using the multi-GNSS differential code bias (DCB) products provided by the German aerospace center. The phase delay at each frequency is assumed to be small floating-point constants. The noise was simulated as white noise, with the standard deviations (STDs) of 0.3 m and 0.003 m for the code and phase observations, respectively. To investigate the contribution of multi-frequency LEO observations to the PPP ambiguity resolution, the LEO observations were simulated at three frequencies: L1 at 1575.42 MHz, L2 at 1227.6 MHz, and L5 at 1176.45 MHz, which is consistent with the current GPS signals.

### *2.2. Multi-Frequency LEO-Augmented PPP AR Method*

To achieve the multi-frequency LEO-augmented PPP ambiguity resolution, the extra-wide-lane, wide-lane, and narrow-lane UPD corrections of GNSS and LEO satellites should be estimated first. The float extra-wide-lane and wide-lane ambiguities ($\overline{N}^s_{r,ewl}$ and $\overline{N}^s_{r,wl}$) can be calculated by the Melbourne-Wübbena (MW, [34,35]) combinations, and the float narrow-lane ambiguities ($\overline{N}^s_{r,nl}$) can be derived from the integer wide-lane ambiguities and ionosphere-free ambiguities. The calculation formulation of extra-wide-lane, wide-lane, and narrow-lane ambiguities can be expressed as follows:

$$\begin{aligned} \overline{N}^s_{r,ewl} &= \left(\frac{L^s_{r,2}}{\lambda_2} - \frac{L^s_{r,3}}{\lambda_3} - \frac{f_2 P^s_{r,2} + f_3 P^s_{r,3}}{(f_2+f_3)\lambda_{ewl}}\right) \\ &= N^s_{r,ewl} + d_{r,ewl} - d^s_{ewl} \end{aligned} \quad (3)$$

$$\begin{aligned} \overline{N}^s_{r,wl} &= \left(\frac{L^s_{r,1}}{\lambda_1} - \frac{L^s_{r,2}}{\lambda_2} - \frac{f_1 P^s_{r,1} + f_2 P^s_{r,2}}{(f_1+f_2)\lambda_{wl}}\right) \\ &= N^s_{r,wl} + d_{r,wl} - d^s_{wl} \end{aligned} \quad (4)$$

$$\begin{aligned} \lambda_{nl} \cdot \overline{N}^s_{r,nl} &= \lambda_{IF} \cdot \overline{N}^s_{r,IF} - \frac{cf_2}{{f_1}^2 - {f_2}^2} \cdot N^s_{r,wl} \\ &= N^s_{r,nl} + d_{r,nl} - d^s_{nl} \end{aligned} \tag{5}$$

where $N^s_{r,ewl}$, $N^s_{r,wl}$ and $N^s_{r,nl}$ are integer extra-wide-lane, wide-lane, and narrow-lane ambiguities, respectively; $\lambda_{ewl}$, $\lambda_{wl}$ and $\lambda_{nl}$ denote the wavelength of the extra-wide-lane, wide-lane, and narrow-lane ambiguities, which can be written as $\lambda_{ewl} = \frac{c}{f_2 - f_3}$, $\lambda_{wl} = \frac{c}{f_1 - f_2}$ and $\lambda_{nl} = \frac{c}{f_1 + f_2}$; $\overline{N}^s_{r,IF}$ denotes ionosphere-free ambiguity and $\lambda_{IF}$ refers to the corresponding wavelength; and $d_{r,ewl}$, $d_{r,wl}$ and $d_{r,nl}$ denote extra-wide-lane, wide-lane, and narrow-lane UPDs at the receiver side, respectively, whereas $d^s_{ewl}$, $d^s_{wl}$ and $d^s_{nl}$ denote the corresponding satellite UPDs. Based on the ambiguities from a global MGEX tracking network, the extra-wide-lane, wide-lane, and narrow-lane UPDs can be precisely estimated with the method of least squares estimation [7,36].

We estimated the extra-wide-lane and wide-lane UPDs as constant during a whole day since the extra-wide-lane and wide-lane UPDs barely change over several months [37], while the narrow-lane UPD is estimated epoch by epoch considering its temporal characteristic [3]. Several specific issues of the UPD estimation for each system should be mentioned. To avoid the influence of the GLONASS inter-frequency biases on the UPD estimation, stations with homogeneous receivers should be employed to estimate the GLONASS UPD. Since the observation of LEO is designed to have the same frequencies of GPS, we can ignore the inter-system biases between these two systems in the UPD estimation. With the improvement of model precision of observations, the fractional parts of narrow-lane ambiguities are relatively stable and can be forecasted for a few hours. Thus, in the process of narrow-lane UPD estimation, if the satellite cannot be observed at this epoch at a station, the fractional parts of ambiguities at the last epoch will be used for narrow-lane UPD estimation to ensure that enough observations are made.

With the UPD corrections, the multi-frequency LEO-augmented PPP AR was achieved by fixing extra-wide-lane, wide-lane, and narrow-lane ambiguities step by step. The satellite UPDs can be removed by the UPD products, while the receiver UPDs of extra-wide-lane and wide-lane ambiguities were obtained by averaging fractional parts of ambiguities with the satellite UPDs corrected. After the removal of the UPDs, the extra-wide-lane ($N^s_{ewl}$) and wide-lane ($N^s_{wl}$) ambiguities were fixed by a rounding strategy [38]. With the long wavelength, the extra-wide-lane and wide-lane ambiguity can be fixed to an integer very efficiently, and the integer extra-wide-lane and wide-lane ambiguities will then formulate an ambiguity-fixed ionosphere-free wide-lane measurement ($P^s_{r,AFIF}$, [14]), which can be expressed as Equation (6).

$$P^s_{r,AFIF} = \frac{f_1}{f_1 - f_3} L^s_{r,w} - \frac{f_3}{f_1 - f_3} L^s_{r,e} - \lambda_{wl} \frac{f_1}{f_1 - f_3} (N^s_{wl} + d_{r,wl} - d^s_{wl}) \tag{6}$$

with

$$L^s_{r,w} = \frac{f_1}{f_1 - f_2} L^s_{r,1} - \frac{f_2}{f_1 - f_2} L^s_{r,2} \tag{7}$$

$$L^s_{r,e} = \frac{f_2}{f_2 - f_3} L^s_{r,2} - \frac{f_3}{f_2 - f_3} L^s_{r,3} - \lambda_{ewl} (N^s_{r,ewl} + d_{r,ewl} - d^s_{ewl}) \tag{8}$$

The ambiguity-fixed ionosphere-free observation formulated by phase observations and fixed extra-wide-lane and wide-lane ambiguities can be regarded as a high-precision code measurement to enable rapid convergence for an ambiguity-float solution. As shown in Equation (5), the narrow-lane ambiguities are derived from the float ionosphere-free ambiguities and integer wide-lane ambiguities, and the rapid convergence of a float solution can also improve the efficiency of narrow-lane ambiguity resolution. For the narrow-lane ambiguity resolution, the satellite UPDs were corrected based on UPD products, while the receiver UPDs were eliminated by the cross-satellite single-difference method. Then, the LAMDA method was applied to fix the between-satellite narrow-lane ambiguity [31,32]. The ratio test with the threshold of 2 was used to validate the effectiveness of the ambiguity resolution. The inclusion of LEO satellites significantly increases the number of candidate ambiguities; however,

it also makes it difficult for the users to fix all ambiguities. Therefore, the partially fixed integer solution was introduced for rapid ambiguity resolution [39].

To conduct the PPP test, observations of 37 globally distributed MGEX stations were selected. Twenty-nine stations denoted by blue dots in Figure 2 were used for UPD estimation and the other eight stations denoted by red dots were selected as user stations. At the user end, daily observables were separated into 24 1-hour-long observable sessions for experiments. The sampling interval was 5 s and the cutoff elevation was set as 7°. An elevation-dependent weighting strategy was applied for ambiguity-fixed PPP, with the carrier noise set to 3 mm and the pseudorange noise set to 0.3 m for each system.

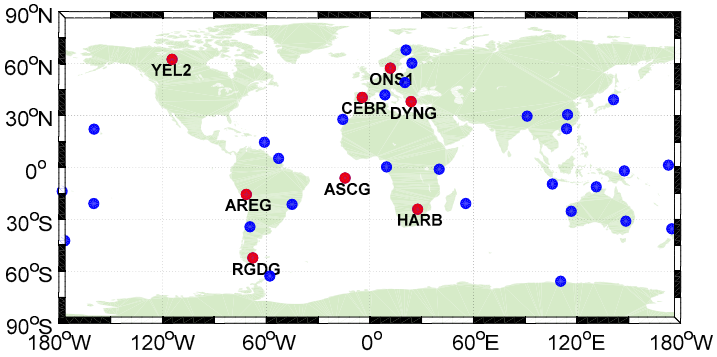


**Figure 2.** Distribution of MGEX stations used for UPD estimation and PPP ambiguity resolution. The blue dots indicate the reference stations, while the red dots denote the user stations.

## 3. Results

### *3.1. UPD Results*

The UPD product is an important premise of PPP ambiguity resolution. In this section, we present the wide-lane and narrow-lane UPDs of GPS, GLONASS, Galileo, BDS, and LEO satellites and analyze the temporal characteristic and residual distribution of UPD products. Note that the LEO UPDs presented in this section were estimated based on observations of the 288-LEO constellation.

Figure 3 shows the narrow-lane UPD series of GPS, GLONASS, Galileo, BDS, and LEO satellites on DOY 001, 2017. We selected seven exemplary satellites of each system and their UPD series are presented in the figure with different colors. It can be seen that the narrow-lane UPD series are quite stable, with the variation of fewer than 0.3 cycles for each system. We further calculated the average STDs of all satellites. The average STDs of GPS, GLONASS, Galileo, BDS, and LEO are 0.035, 0.068, 0.016, 0.026, and 0.014 cycles, respectively. The average STDs of UPD products are all less than 0.1 cycles, which indicates the high temporal stability of estimated narrow-lane UPD products.

The posterior residual, which can be regarded as the fractional parts of ambiguities after the removal of UPDs, is an important indicator to investigate the quality of the UPD products [40]. Figure 4 presents the wide-lane residual distribution of GPS, GLONASS, Galileo, BDS, and LEO. The average value of wide-lane residuals of each system is close to zero, which indicates that there are no additional systematic biases after the removal of UPDs. With the fixing criteria of 0.15 cycles, the fixing percentage is greater than 90% for all systems. The narrow-lane residual distribution is shown in Figure 5. The fixing percentages within 0.15 cycles are 85.2%, 79.6%, 97.3%, 90.1%, and 84.8% for GPS, GLONASS, Galileo, BDS, and LEO satellites, respectively. Additionally, the STDs are also given in Figure 5, which are no more than 0.35 cycles for all systems. It can be seen that the UPDs of LEO present a comparable performance to GNSS UPDs, which is expected to achieve ambiguity resolution effectively.

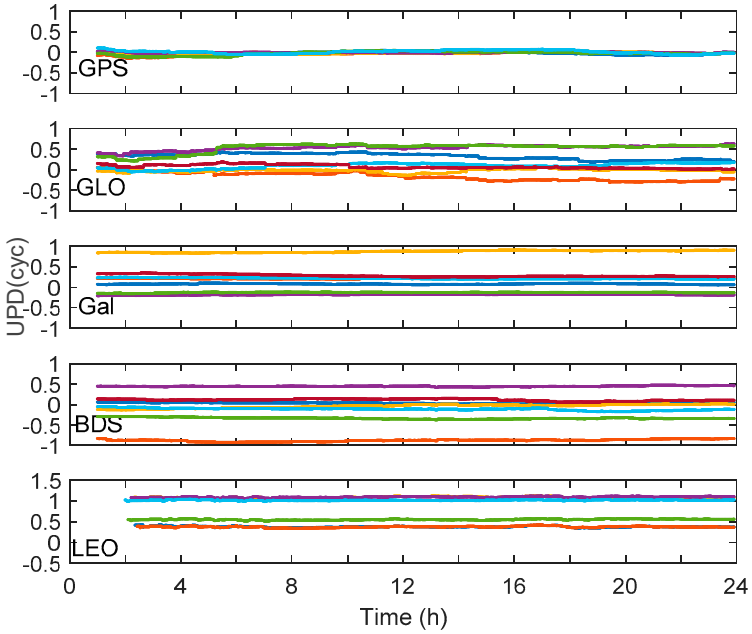


**Figure 3.** Narrow-lane UPD series of GPS, GLONASS, Galileo, BDS, and LEO on DOY 001, 2017. The abbreviations GLO and Gal indicate the GLONASS and Galileo, respectively.

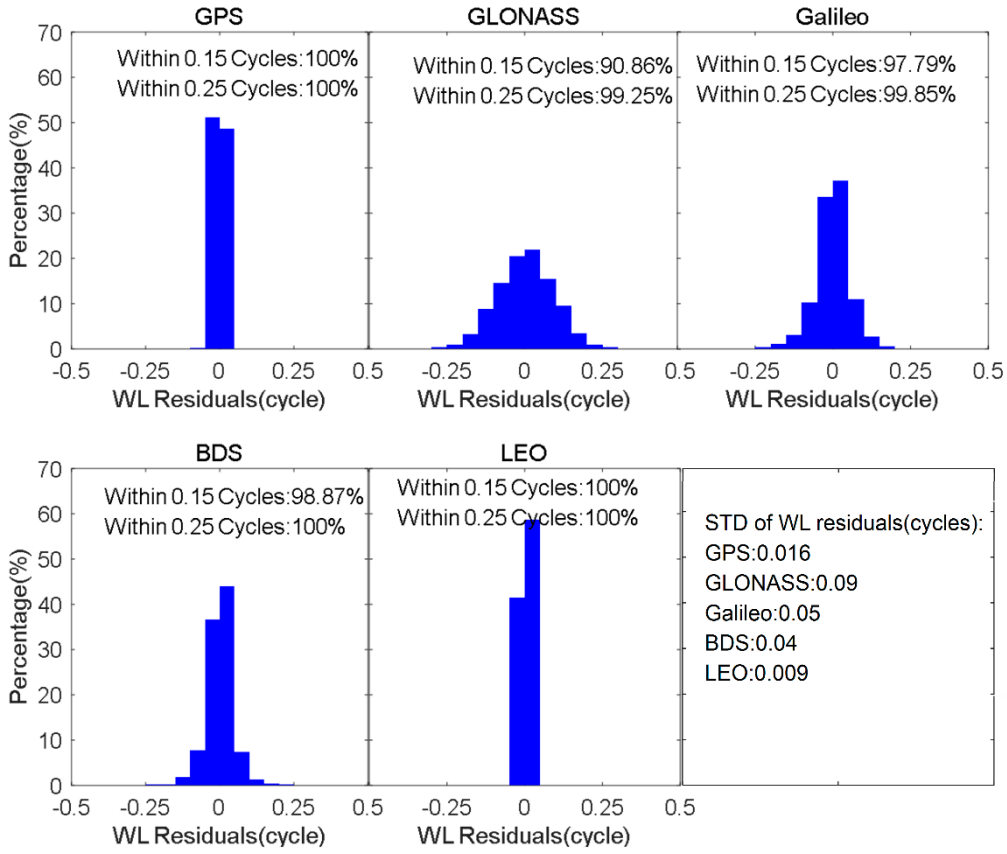


**Figure 4.** Residual distribution of wide-lane UPDs for GPS, GLONASS, Galileo, BDS, and LEO.

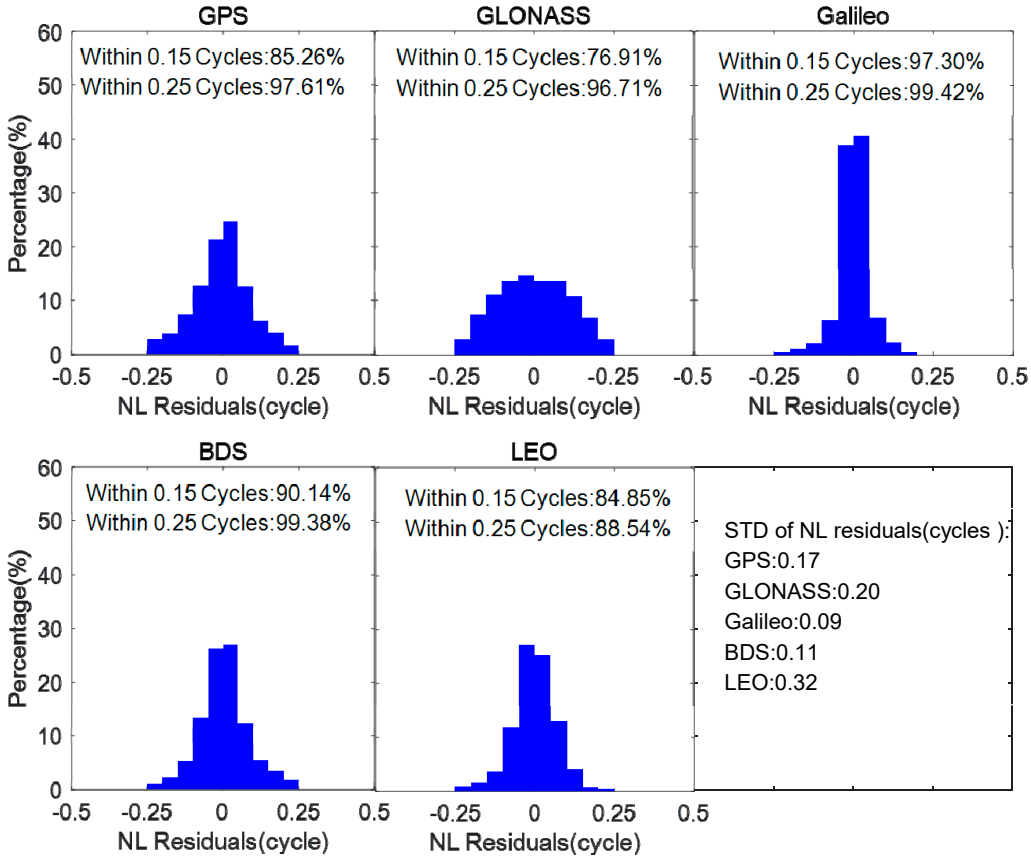


**Figure 5.** Residual distribution of narrow-lane UPDs for GPS, GLONASS, Galileo, BDS, and LEO.

### *3.2. PPP AR with the Augmentation of Multi-Frequency LEO Observation*

With the stable UPD products of GNSS and LEO, LEO-augmented PPP ambiguity resolution can be achieved. The augmentation performance with different LEO constellations was evaluated by first introducing three types of LEO constellation consisting of 60, 192, and 288 LEO satellites, respectively. For the purpose of investigating the contribution of multi-frequency LEO observation to ambiguity resolution, three solutions, including the dual-frequency PPP float solution (Float), dual-frequency PPP fixed solution (DF_fixed), and triple-frequency PPP fixed solution (TF_fixed), were analyzed and compared. Note that in the processing of triple-frequency PPP AR, only triple-frequency LEO observations are employed, while dual-frequency GNSS observations are used.

#### 3.2.1. PPP AR with the Different LEO Constellation

Figure 6 shows the positioning errors of GPS, BDS, and GREC PPP fixed solutions at station ASCG on 1 January 2017. The blue, green, and red lines refer to the results of GPS, BDS, and GREC, respectively. For single-system PPP ambiguity resolution, it takes about 30 min to achieve an accuracy of millimeter-level in all three components. Compared to the single-system PPP AR, the GREC PPP AR presents obviously faster convergence. It requires approximately 8 min to achieve the first fix.

The inclusion of LEO constellation can shorten the convergence of the PPP float solutions, which has been proved in previous studies [14,15]. It is anticipated that the PPP ambiguity resolution can also be improved with the augmentation of LEO satellites. The static GREC PPP fixed solutions with the inclusion of 0, 60, 192, and 288 LEO satellites at stations ASCG, CEBR, and YEL2 are shown in Figure 7. It can be obviously found that the inclusion of LEO satellites can significantly shorten the initialization time of multi-GNSS PPP AR. Furthermore, a shorter initialization time can be achieved with more visible LEO satellites. With observations of the 288-LEO constellation, the GREC fixed solutions can converge to 5 cm in all three directions within 1 minute for all three stations. The corresponding total

numbers of visible satellites (NSAT) and the position dilution of precision (PDOP) values are also shown in Figure 7, respectively. Taking the YEL2 station as an example, the average NSAT and PDOP are 35.6 and 0.8 for the GREC solution. With the augmentation of 60-, 196-, and 288-LEO constellations, the corresponding NSATs increase by 4.6, 13.3, and 19.9, respectively, while the averaged PDOP values decrease to 0.78, 0.70, and 0.66, respectively. In addition, the NSAT and PDOP values change quickly with the inclusion of LEO satellites. The results demonstrated that the inclusion of LEO constellation can increase visible satellites and optimize the spatial geometry, which is beneficial for the rapid ambiguity resolution of PPP.

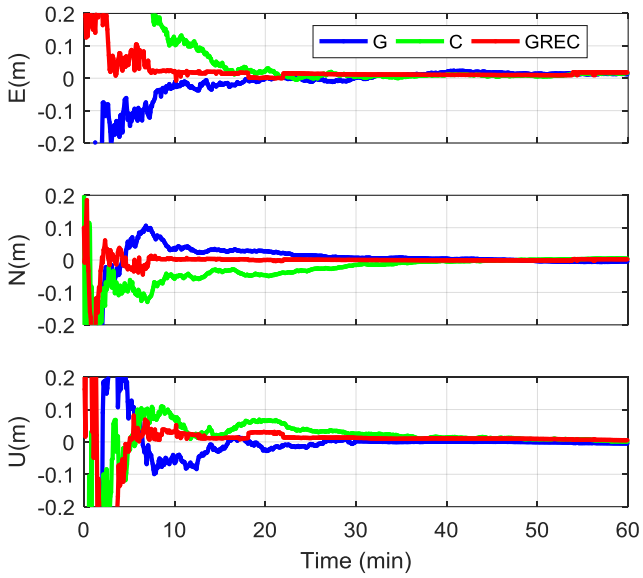


**Figure 6.** Static PPP AR solutions of GPS, BDS, and multi-GNSS (GREC) at station ASCG from 19:00 to 20:00 on 1 January 2017.

The averaged TTFF of LEO-augmented PPP fixed solutions of all user stations was calculated and the corresponding results are shown in Table 1. We can see that the inclusion of LEO satellites can significantly shorten the TTFF for single- and multi-GNSS PPP ambiguity resolution and more LEO satellites will contribute to shorter TTFF. The TTFF of GPS-only and BDS-only PPP ambiguity resolution is 17 and 15.9 min, respectively, which can be improved to 0.94 and 0.99 min with the augmentation of 288-LEO constellation, with the improvement of 94.4% and 93.7%, respectively. As for the GREC fixed solutions, the TTFF can be shortened from 7.1 to 4.8, 1.1, and 0.7 min by introducing observations of 60-, 192-, and 288-LEO constellations. With the augmentation of the 288-LEO constellation, the TTFF values of GPS, BDS, and GREC PPP AR are all less than 1 min. Moreover, for GREC PPP AR, with the 288 LEO satellites, it only takes about 40s to achieve the first ambiguity resolution.

**Table 1.** TTFF of GPS, BDS, and GREC PPP AR without or with the augmentation of 60, 192, and 288 LEO satellites (unit: min).

| LEO Satellites | GPS | | BDS | | GREC | |
|---|---|---|---|---|---|---|
| | **TTFF** | **Reduction** | **TTFF** | **Reduction** | **TTFF** | **Reduction** |
| 0 | 17 | 0% | 15.9 | 0% | 7.1 | 0% |
| 60 | 7.4 | 56.4% | 6.4 | 59.7% | 4.8 | 32.3% |
| 192 | 1.4 | 91.7% | 1.3 | 91.6% | 1.09 | 84.6% |
| 288 | 0.94 | 94.4% | 0.99 | 93.7% | 0.70 | 90.1% |

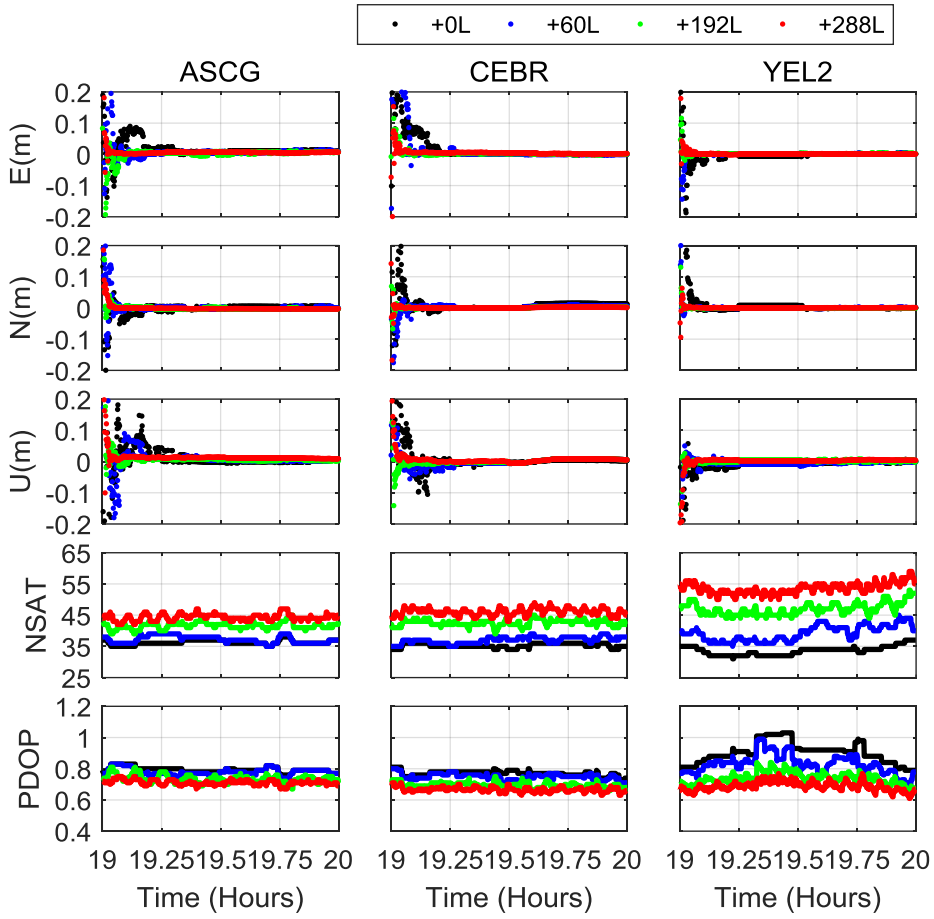


**Figure 7.** Comparisons of LEO-augmented multi-GNSS PPP fixed solutions with different LEO constellations at stations ASCG, CEBR, and YEL2. The corresponding NSAT and PDOP are also shown in the figure.

In order to investigate the position accuracy of the LEO-augmented PPP ambiguity resolution, the positioning errors of static PPP with different session lengths (1 min, 5 min, 10 min, and 30 min) were calculated. Figure 8 shows the statistical results of the GREC PPP fixed solutions with the inclusion of 0, 60, 192, and 288 LEO satellites. With the augmentation of the LEO satellites, the positioning accuracy of GNSS PPP can be significantly improved and the improvement is more remarkable when more LEO satellites are added. At the 1 min-observation session, the positioning accuracies of GREC-only and 60-LEO augmented PPP fixed solutions are greater than 8 cm in three components, while the positioning accuracy of 192-LEO and 288-LEO augmented GNSS fixed solutions can be 3–4 cm in the horizontal components and 4–6 cm in the vertical components. At the 5 min-observation session, the positioning accuracy of multi-GNSS fixed solutions is improved by about 60%, 80%, and 90% from (3.5, 1.8, 4.9) cm to (1.8, 0.6, 2.6) cm, (0.70, 0.23, 1.4) cm, and (0.34, 0.21, 1.34) cm in east, north, and up components, with the inclusion of 60, 192, and 288 LEO satellites, respectively. We are glad to see that, with the augmentation of 192 and 288 satellites, a centimeter-level accuracy can be achieved within 1 min, while a millimeter-level accuracy in the horizontal direction can be achieved within 5 min for GNSS PPP AR.

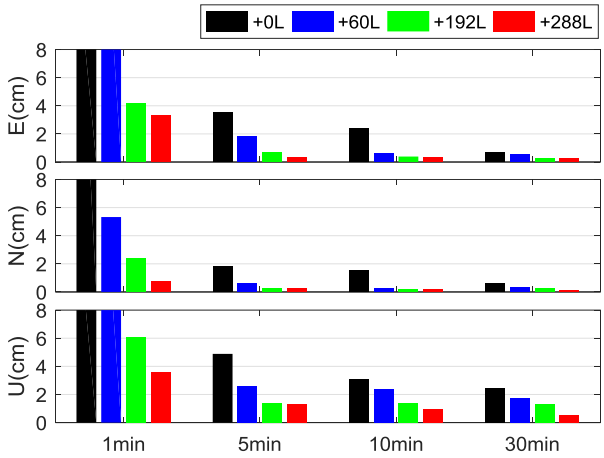


**Figure 8.** Positioning accuracy of static GREC PPP fixed solutions with different session lengths (1 min, 5 min, 10 min, and 30 min) with the augmentation of 0, 60, 192, and 288 LEO satellites.

### 3.2.2. PPP AR with the Triple-Frequency LEO Observation

To evaluate the benefits of triple-frequency LEO observations for PPP rapid ambiguity resolution, triple-frequency PPP fixed solutions with the augmentation of 288 LEO-constellation were conducted. Figure 9 shows the PPP fixed solutions with the augmentation of the dual- and triple-frequency LEO observations within 5 min at stations CEBR, ASCG, and DYNG. As expected, the ambiguities were fixed within 1 min for dual-frequency PPP AR and the positioning accuracy was significantly improved once the ambiguities were fixed to the correct integers. The triple-frequency PPP AR can converge to a sub-meter level instantaneously, which presents a faster convergence and higher positioning accuracy compared to the dual-frequency fixed solutions.

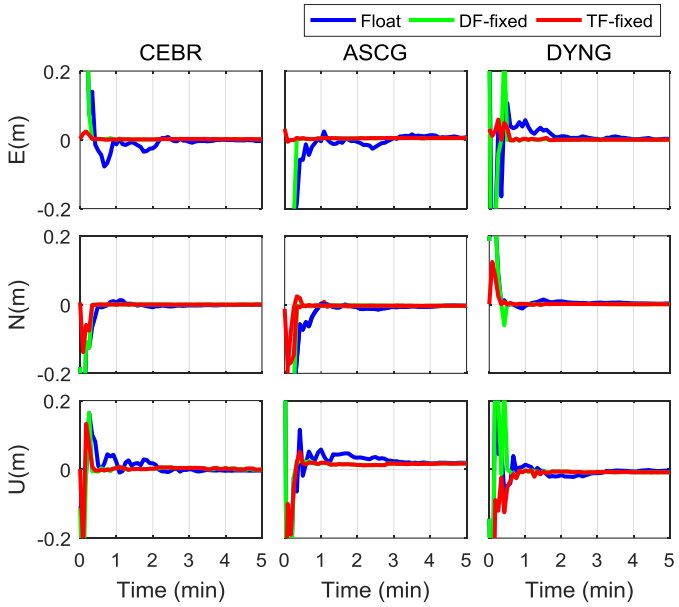


**Figure 9.** PPP fixed solutions with the augmentation of the dual- and triple-frequency observations of the 288-LEO constellation.

The average TTFF values of dual-frequency and triple-frequency fixed solutions were calculated and plotted in Figure 10. It can be seen that, with the augmentation of 288-LEO constellation, the time to first fix of each user station is less than 60 s. After the inclusion of the third frequency of LEO, it only requires 33 s to achieve the first fix.

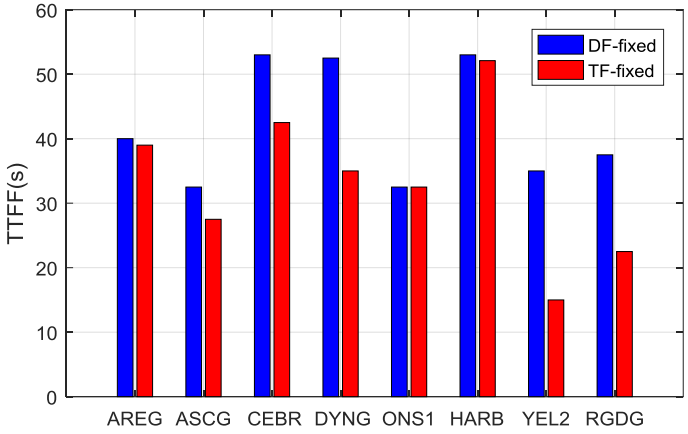


**Figure 10.** Average TTFF of the 288-LEO augmented GNSS PPP AR at dual-frequency and triple-frequency modes.

### *3.3. Multi-Frequency LEO-Only PPP AR*

To verify the capability of LEO constellation for precise positioning independently, we conducted the LEO-only PPP test in dual-frequency and triple-frequency modes based on the observation of 288-LEO constellation. Figure 11 shows LEO-only PPP float and fixed solutions at stations CEBR, AREG, and DYNG from 20:00 to 20:05 on 1 January 2017. According to Figure 11, the LEO-only PPP can converge to a centimeter level in all three components within 5 min and the ambiguity resolution can be achieved in a very short period, which is about 2 min. Compared to the dual-frequency LEO-only fixed solutions, the triple-frequency PPP fixed solutions present a better performance in terms of convergence and reliability.

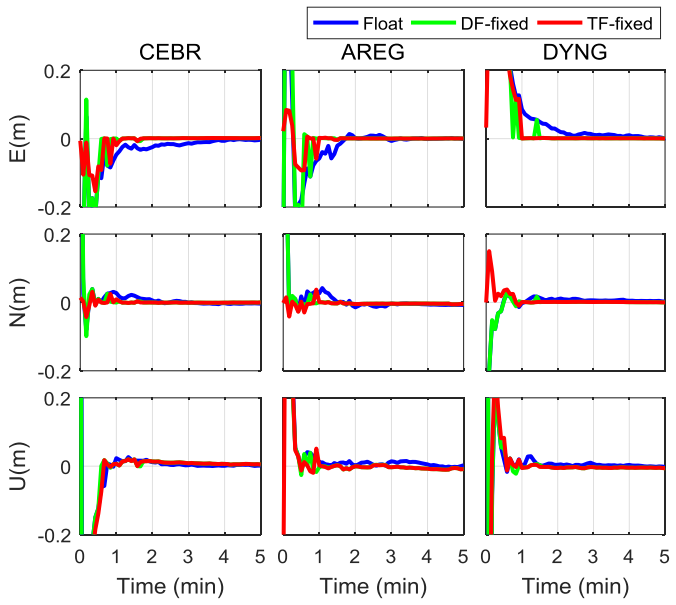


**Figure 11.** LEO-only PPP float and fixed solutions at stations AREG, CEBR, and RGDG from 20:00 to 20:05 on 1 January 2017.

Figure 12 presents the average TTFF of the LEO-only PPP AR for all user stations. For dual-frequency solutions, the TTFF is less than 100 s, except for the station AREG, and the average TTFF is 71.8 s, which is obviously less than the TTFF of the GREC PPP AR of about 7.1 min, which is benefited by the rapid change of spatial geometry of LEO satellites. The TTFF of the triple-frequency

PPP AR is less than 80 s for all user stations and the average TTFF is 55.2 s, with an improvement of 23.1% compared to the dual-frequency solutions.

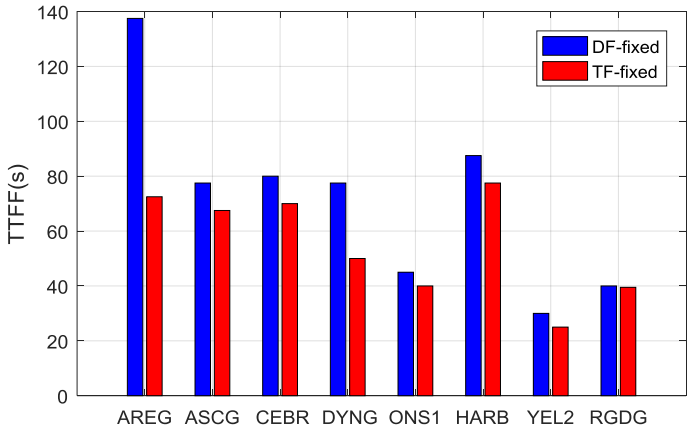


**Figure 12.** TTFF of LEO-only PPP AR for each user station.

The positioning errors of 1-min static LEO-only float and fixed solutions are given in Figure 13. The positioning accuracy of LEO-only solutions can converge to 6 cm in all three components within 1 min. With the ambiguities fixed, the 1-min positioning accuracy can be significantly improved. The positioning error of triple-frequency PPP AR at 1 min is (1.69, 0.75, 4.16) cm in the east, north, and up components, respectively, with an improvement of 63.2%, 67.2%, and 20.7% compared to the PPP float solutions, and 50.2%, 56.8%, and 17.2% compared to the dual-frequency PPP fixed solutions. It also demonstrates the benefit of the third frequency for PPP ambiguity resolution.

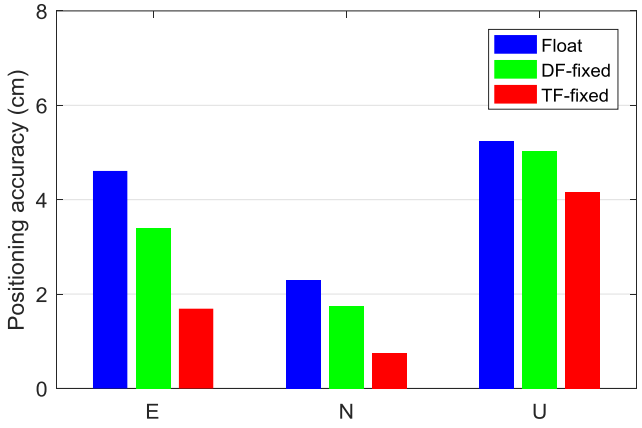


**Figure 13.** Positioning accuracy of 1-min static LEO-only float and fixed solutions.

## 4. Discussions

The long initialization time is still a serious problem of PPP, which limits the wider application of PPP in some time-critical applications. The fast motion of LEO satellites contributes to geometry diversity, allowing for the rapid convergence of PPP [21–23]. Since the previous studies focused on the contribution of LEO constellation to dual-frequency GNSS float solutions, in this contribution, we investigated the PPP rapid ambiguity resolution with the augmentation of LEO constellations and the triple-frequency observation data was fully exploited to further improve the performance of ambiguity resolution. The results demonstrated that the TTFF of the GREC fixed solution can be shortened from 7.1 to 4.8, 1.1, and 0.7 min and the positioning accuracy can be improved by about 60%, 80%, and 90% with the augmentation of 60, 192, and 288 LEO satellites, respectively. Moreover, the TTFF of 288-LEO augmented GREC solutions can be shortened to 33 s with triple-frequency

observations. The joint of the third frequency brings more combinations to assist the narrow-lane ambiguity resolution, which can further improve the performance of the PPP AR. The 288-LEO constellation has the capability of achieving high-precision positioning independently, with the average TTFF of 71.8 s and 55.2 s in dual-frequency and triple-frequency modes, respectively. Since the LEO constellation is still in the demonstration stage or under construction, the contribution of multiple LEO-constellations and signals to PPP AR was investigated based on the simulation data. With more and more LEO satellites available, it is necessary to assess the augmentation performance of LEO based on the measured data.

The fusion of GNSS and LEO constellation can significantly increase the number of observed satellites; optimize the spatial geometry; and improve the convergence, accuracy, continuity, and reliability of precise positioning. Especially, the multi-frequency signals of LEO constellation bring new opportunities for rapid ambiguity resolution. In the sequential studies, the observations of different LEO constellations with different orbit altitudes and types (such as a combination of equatorial and polar circular orbits) should be fully exploited to further improve the multi-GNSS performance. In addition, the LEO constellation not only enhances precise positioning applications, but can also provide a high-resolution (time and space) observable for monitoring of the neutral atmosphere, which might be highly valuable for meteorological applications such as now-casting of severe weather events or regional short-term forecast systems.

## 5. Conclusions

This paper investigated the performance of PPP ambiguity resolution with the augmentation of different LEO constellations. The contribution of triple-frequency observation of LEO to ambiguity resolution was also analyzed. Based on the simulated observation data for ground stations, the UPD products of the GNSS and LEO satellites were estimated and the temporal characteristic, as well as residuals distribution, were analyzed. With the UPD products, the LEO-augmented PPP ambiguity resolution was achieved and the performance in terms of time to first fix and positioning accuracy was also evaluated.

Observations of 29 global distributed MGEX stations were employed for UPD estimation. The resultant narrow-lane UPD products showed a high temporal stability during a whole day, with the average STD being less than 0.1 cycles. The residual distributions of five systems (GPS, GLONASS, Galileo, BDS, and LEO) were all close to a normal distribution, with the mean value of zero. With the fixing criteria of 0.15 cycles, the fixing percentage of wide-lane and narrow-lane ambiguity was greater than 90% and 80% for each system, respectively. With stable UPD products, a PPP ambiguity resolution using the LEO and GNSS observations can be achieved. The performance of multi-GNSS PPP AR can be significantly improved with the augmentation of LEO satellites and more LEO satellites contribute to a better performance. The TTFF of GREC PPP AR can be shortened from 7.1 to 4.8, 1.1, and 0.7 min by introducing observations from 60, 192, and 288 LEO satellites, respectively. The positioning accuracy of multi-GNSS fixed solutions is improved by about 60%, 80%, and 90% with the inclusion of 60, 192, and 288 LEO satellites, respectively. Moreover, a millimeter-level accuracy in the horizontal direction can be achieved within 5 min for GNSS PPP AR with the augmentation of 192 and 288 satellites. The improvement of the PPP performance benefits from the augmentation of the LEO constellation, which increases the number of visible satellites, optimizes the spatial geometry, and provides more candidate ambiguities to be resolved.

The multiple signals of LEO satellites bring a variety of combinations applied for accelerating ambiguity resolution. With the inclusion of 288-LEO constellation, the triple-frequency LEO-augmented triple-frequency PPP AR was conducted. Compared to the dual-frequency fixed solutions, the triple-frequency AR achieved a faster convergence and higher positioning accuracy. The TTFF of the LEO-augmented GREC PPP AR was shortened from 42 s to 33 s. The multi-frequency LEO-only PPP AR was explored for the first time based on 288-satellite LEO constellation. The TTFF of the triple-frequency PPP AR was less than 80 s for all user stations and the average TTFF was 55.2 s,

with an improvement of 23.1% compared to the dual-frequency solutions. The positioning error of triple-frequency PPP AR at 1 min was (1.69, 0.75, 4.16) cm in the east, north, and up components, respectively, with an improvement of 63.2%, 67.2%, and 20.7% compared to the PPP float solutions, and 50.2%, 56.8% and 17.2% compared to the dual-frequency PPP fixed solutions. We are glad to see that the inclusion of the LEO constellation will bring great improvement for the PPP AR and the multiple signals of LEO satellites will provide more possibilities for improving the efficiency of ambiguity resolution.

**Author Contributions:** X.L. (Xin Li), X.L. (Xingxing Li), and F.M. conceived and designed the experiments; X.L. (Xin Li), X.L. (Xingxing Li), and F.M. performed the experiments, analyzed the data, drew pictures, and wrote the paper; Y.Y., K.Z., F.Z., and X.Z. reviewed the paper.

**Funding:** This research was funded by the National Natural Science Foundation of China (Grant No. 41774030), National Science Fund for Distinguished Young Scholars (Grant No. 41825009), the Hubei Province Natural Science Foundation of China (Grant No. 2018CFA081), and the National Youth Thousand Talents Program.

**Acknowledgments:** We would like to express our gratitude to IGS-MGEX for providing multi-GNSS data and products, as well as the help from Mohamed Freeshah.

**Conflicts of Interest:** The authors declare no conflict of interest.

## References

1. Zumberge, J.F.; Heflin, M.B.; Jefferson, D.C.; Watkins, M.M.; Webb, F.H. Precise point positioning for the efficient and robust analysis of GPS data from large networks. *J. Geophys. Res. Solid Earth* **1997**, *102*, 5005–5017. [CrossRef]
2. Witchayangkoon, B. Elements of GPS precise point positioning. In *Spatial Information Science and Engineering*; University of Maine: Orono, ME, USA, 2000.
3. Ge, M.; Gendt, G.; Rothacher, M.; Shi, C.; Liu, J. Resolution of GPS carrier phase ambiguities in precise point positioning (PPP) with daily observations. *J. Geod.* **2008**, *82*, 389–399. [CrossRef]
4. Collins, P.; Lahaye, F.; Herous, P.; Bisnath, S. Precise point positioning with AR using the decoupled clock model. In Proceedings of the ION GNSS 2008, Savannah, GA, USA, 16–19 September 2008; pp. 1315–1322.
5. Geng, J.; Teferle, F.N.; Shi, C.; Meng, X.; Dodson, A.H.; Liu, J. Ambiguity resolution in precise point positioning with hourly data. *GPS Solut.* **2009**, *13*, 263–270. [CrossRef]
6. Laurichesse, D.; Mercier, F.; Berthias, J.P.; Broca, P.; Cerri, L. Integer ambiguity resolution on undifferenced GPS phase measurements and its application to PPP and satellite precise orbit determination. *Navigation* **2009**, *56*, 135–149. [CrossRef]
7. Li, X.; Zhang, X. Improving the estimation of uncalibrated fractional phase offsets for PPP ambiguity resolution. *Navigation* **2012**, *65*, 513–529. [CrossRef]
8. Li, X.; Li, X.; Yuan, Y.; Zhang, K.; Zhang, X.; Wickert, J. Multi-GNSS phase delay estimation and PPP ambiguity resolution: GPS, BDS, GLONASS, Galileo. *J. Geod.* **2018**, *92*, 579–608. [CrossRef]
9. Li, X.; Ge, M.; Dai, X.; Ren, X.; Fritsche, M.; Wickert, J.; Schuh, H. Accuracy and reliability of multi-GNSS real-time precise positioning: GPS, GLONASS, BeiDou, and Galileo. *J. Geod.* **2015**, *89*, 607–635. [CrossRef]
10. Shi, C.; Zhao, Q.; Li, M.; Tang, W.; Hu, Z.; Lou, Y.; Liu, J. Precise orbit determination of Beidou Satellites with precise positioning. *Sci. China Earth Sci.* **2012**, *55*, 1079–1086. [CrossRef]
11. Cai, C.; Gao, Y. Modeling and assessment of combined GPS/GLONASS precise point positioning. *GPS Solut.* **2013**, *17*, 223–236. [CrossRef]
12. Li, P.; Zhang, X. Integrating GPS and GLONASS to accelerate convergence and initialization times of precise point positioning. *GPS Solut.* **2014**, *18*, 461–471. [CrossRef]
13. Li, X.; Zhang, X.; Ren, X.; Fritsche, M.; Wickert, J.; Schuh, H. Precise positioning with current multi-constellation global navigation satellite systems: GPS, GLONASS, Galileo and BeiDou. *Sci. Rep.* **2015**, *5*, 8328. [CrossRef]
14. Geng, J.; Bock, Y. Triple-frequency GPS precise point positioning with rapid ambiguity resolution. *J. Geod.* **2013**, *87*, 449–460. [CrossRef]
15. Gu, S.; Lou, Y.; Shi, C.; Liu, J. Beidou phase bias estimation and its application in precise point positioning with triple-frequency observable. *J. Geod.* **2015**, *89*, 979–992. [CrossRef]

16. Li, P.; Zhang, X.; Ge, M.; Schuh, H. Three-frequency BDS precise point positioning ambiguity resolution based on raw observables. *J. Geod.* **2018**, *92*, 1357–1369. [CrossRef]
17. Li, X.; Li, X.; Liu, G.; Feng, G.; Yuan, Y.; Zhang, K.; Ren, X. Triple-frequency PPP ambiguity resolution with multi-constellation GNSS: BDS and Galileo. *J. Geod.* **2019**. [CrossRef]
18. Selding PBD. SpaceX to Build 4000 Broadband Satellites in Seattle. Space News Website. 2015. Available online: http://spacenews.com/spacex-opening-seattle-plant-to-build-4000-broadband-satellites/ (accessed on 19 January 2015).
19. Selding PBD. Virgin, Qualcomm Invest in OneWeb Satellite Internet Venture. Space News Website. 2015. Available online: http://spacenews.com/virgin-qualcomm-invest-in-global-satellite-internet-plan/ (accessed on 15 January 2015).
20. Selding, P.B. Boeing Proposes Big Satellite Constellations in V- and C-bands. Space News Website. 2016. Available online: http://spacenews.com/boeing-proposes-big-satellite-constellations-in-v-and-c-bands/ (accessed on 23 June 2016).
21. Enge, P.; Ferrell, B.; Bennet, J.; Whelan, D.; Gutt, G.; Lawrence, D. Orbital Diversity for Satellite Navigation. In Proceedings of the 25th International Technical Meeting of the Satellite Division of The Institute of Navigation (ION GNSS 2012), Nashville, TN, USA, 17–21 September 2012; pp. 3834–3846.
22. Ke, M.; Lv, J.; Chang, J.; Dai, W.; Tong, K.; Zhu, M. Integrating GPS and LEO to accelerate convergence time of precise point positioning. In Proceedings of the 7th International Conference on Wireless Communications and Signal Proceeding (WCSP), Nanjing, China, 15–17 October 2015; pp. 1–5.
23. Ge, H.; Li, B.; Ge, M.; Zang, N.; Nie, L.; Shen, Y.; Schuh, H. Initial Assessment of Precise Point Positioning with LEO Enhanced Global Navigation Satellite Systems (LeGNSS). *Remote Sens.* **2018**, *10*, 984. [CrossRef]
24. Li, X.; Ma, F.; Li, X.; Lu, H.; Blan, L.; Jiang, Z.; Zhang, X. LEO constellation-augmented multi-GNSS for rapid PPP convergence. *J. Geod.* **2018**. [CrossRef]
25. Satellite Tool Kit. *Software Package*; Analytical Graphics Inc.: Exton, PA, USA, 2006.
26. DOD SPS. Department of Defense USA. *Global Positioning System Standard Positioning Service Performance Standard*, 4th ed.; 2008. Available online: http://www.gps.gov/technical/ps/2008-SPS-performancestandard (accessed on 6 January 2012).
27. *Global Navigation Satellite System GLONASS–Interface Control Document, v5.1*; Russian Institute of Space Device Engineering: Moscow, Russian, 2008.
28. OS-SIS-ICD. *European GNSS (Galileo) Open Service Signal in Space Interface Control Document*; SISICD-2006; Eur Space Agency: Paris, France, 2010.
29. CSNO. *BeiDou Navigation Satellite System Signal in Space Interface Control Document-Open Service Signal, Version 2.0*; China Satellite Navigation Office: Beijing, China, 2013.
30. Hofmann-Wellenhof, B.; Lichtenegger, H.; Wasle, E. *GNSS: Global Navigation Satellite Systems: GPS, Glonass, Galileo, and more*; Springer: New York, NY, USA, 2008.
31. Saastamoinen, J. Contributions to the theory of atmospheric refraction. *Bulletin Géodésique* **1972**, *105*, 279–298. [CrossRef]
32. Kouba, J. A Guide to Using International GNSS Service (IGS) Products. 2009. Available online: http://igscb.jpl.nasa.gov/igscb/resource/pubs/UsingIGSProductsVer21.pdf (accessed on 15 January 2019).
33. Yizengaw, E.; Moldwin, M.B.; Galvan, D.; Iijima, B.A.; Komjathy, A.; Mannucci, A.J. Global plasmaspheric TEC and its relative contribution to GPS TEC. *J. Atmos. Sol. Terr. Phys.* **2008**, *70*, 1541–1548. [CrossRef]
34. Melbourne, W.G. The case for ranging in GP S-based geodetic systems. In Proceedings of the First International Symposium on Precise Positioning with the Global Positioning System, Rockville, MD, USA, 15–19 April 1985.
35. Wübbena, G. Software developments for geodetic positioning with GPS using TI-4100 code and carrier measurements. In Proceedings of the First International Symposium on Precise Positioning with the Global Positioning System, Rockville, MD, USA, 15–19 April 1985.
36. Ding, W.W.; Teferle, F.N.; Kazmierski, K.; Laurichesse, D.; Yuan, Y.B. An evaluation of real-time troposphere estimation based on gnss precise point positioning. *J. Geophys. Res.-Atmos.* **2017**, *122*, 2779–2790. [CrossRef]
37. Gabor, M.J.; Nerem, R.S. GPS carrier phase AR using satellite single difference. In Proceedings of the ION GNSS 1999, Institute of Navigation, Nashville, TN, USA, 14–17 September 1999; pp. 1569–1578.
38. Dong, D.; Bock, Y. Global positioning system network analysis with phase ambiguity resolution applied to crustal deformation studies in California. *J. Geophys. Res.* **1989**, *94*, 3949–3966. [CrossRef]

39. Teunissen, P.J.G. The least-squares ambiguity decorrelation adjustment: A method for fast GPS integer ambiguity estimation. *J. Geod.* **1995**, *70*, 65–82. [CrossRef]
40. Li, P.; Zhang, X.; Fei, G. Ambiguity resolved precise point positioning with GPS and BeiDou. *J. Geod.* **2016**, *91*, 1–16.